



Effect of Air Bubbles on Heat Transfer Coefficient in Turbulent Convection Flow

Assit.Prof. Akram W. Ezzat
Mechanical Eng. Dept.
University of Baghdad
email: akramwahbi@yahoo.ie

Prof.Dr. Najdat N. Abdullah
Mechanical Eng. Dept.
University of Baghdad
email: najdat_abdulla @yahoo.co.uk

Sajida Lafta Ghashim
Mechanical Eng. Dept.
University of Baghdad
email: sajda_lafta@yahoo.com

ABSTRACT

Experimental and numerical studies have been conducted for the effect of injected air bubbles on the heat transfer coefficient through the water flow in a vertical pipe under the influence of uniform heat flux. The investigated parameters were water flow rate of (10, 14 and 18) lit/min, air flow rate of (1.5, 3 and 4) lit/min for subjected heat fluxes of (27264, 36316 and 45398) W/m². The energy, momentum and continuity equations were solved numerically to describe the motion of flow. Turbulence models k-ε was implemented. The mathematical model is using a CFD code Fluent (Ansys15). The water was used as continuous phase while the air was represented as dispersed phase. The experimental work includes design, build and instrument a test rig for that purpose. A circular vertical copper pipe test section of (length=0.7m, diameter= 0.05m, thickness= 1.5mm) is designed and constructed, heated by an electrical heater fixed on its outer surface. Water temperature at inlet is kept constant at (32°C). Water inlet and outlet temperatures, as well as radial temperature distribution within the pipe at seven sections along it between pipe surface and its center are measured. The results revealed that the secondary flow created by air bubbles have significant effects on heat transfer enhancement and temperature profile. It is observed, that averaged Nusselt number enhancement for low heat flux of 27264 W/m² and 4 lit/min air bubbles was 33.3 % and 23% in numerical and experimental, respectively.

Keywords: turbulent flow, two phase flow, enhancement of heat transfer, air bubbles.

تأثير فقاعات الهواء على معامل انتقال الحرارة في جريان الحمل المضطرب

م. ساجدة لفته غشيم
قسم الهندسة الميكانيكية
جامعة بغداد/ طالبة دكتوراه

أ.د. نجدت نشات عبد الله
قسم الهندسة الميكانيكية
جامعة بغداد

أ.م.د. اكرم وهبي عزت
قسم الهندسة الميكانيكية
جامعة بغداد

الخلاصة: اجريت دراسة عملية ونظرية حول تأثير حقن فقاعات الهواء على معامل انتقال الحرارة خلال جريان الماء في انبواب عمودي تحت تأثير الفيض الحراري المنتظم . والمتغيرات المدروسة كانت قيم معدل تدفق الماء (10, 14, 18) لتر/ دقيقة ، وقيم معدل تدفق الهواء (1.5, 3, 4) لتر/ دقيقة لفيض حراري مقداره (27264, 36316, 45398) واط/ مترمربع .جلت معادلات الزخم والاستمرارية والطاقة عدديا باستخدام البرنامج الجاهز فلونت (انسس 15) لوصف حركة الجريان بالاضافة الى معادلات نموذج الاضطراب . تم بناء منظومة في الجانب العملي تتكون من مجموعة من الاجزاء من ضمنها مقطع الاختبار وهو عبارة عن انبوب عمودي دائري مصنوع من النحاس ومسخنة بواسطة مسخن كهربائي على السطح الخارجي . ابعاد الاسطوانة النحاسية كانت طول 70 سم وقطر 5 سم وسمك 1.5 ملم . تم استخدام الماء بدرجة حرارة دخول ثابتة 32 درجة مئوية . تم قياس درجة حرارة الماء في الدخول والخروج بالاضافة الى قياس درجات الحرارة على طول الانبوب في سبع مقاطع موزعة بين مركز



الاسطوانة والى الجدار. اظهرت النتائج ان وجود فقاعات الهواء تسبب جريان ثانوي داخل مقطع الاختبار له تأثير على تحسين معامل انتقال الحرارة وتوزيع درجات الحرارة. اظهرت النتائج النظرية والعملية انه عند استخدام فيض حراري منخفض 27264 W/m^2 ومعدل تدفق الهواء 4 لتر/ دقيقة تحسن معدل Nusselt number بمقدار 33.3% و23% على التوالي.

الكلمات الرئيسية: الجريان المضطرب ، الجريان الثنائي الطور ، تحسين معامل انتقال الحرارة ، فقاعات الهواء .

1. INTRODUCTION

Multiphase or two phase flow plays an important role in application of enhancement heat transfer such as heat exchangers, chemical reactors, cooling devices, solar collectors and nuclear reactors. Bubble motion close to a wall plays an effective technique for enhanced heat transfer rate. **Kenning, and Kao, 1972**, investigated experimentally the effect of small gas bubbles of (N_2) flowing upward in channel with rectangular cross-section on the convective heat transfer parameters. Superficial air velocity of (0.11, 0.022 and 0.044) m/s and superficial water velocity of (0.6, 1.2 and 1.8) m/s were used in the experiments. The boundary conditions related to applied heat fluxes ranged (20- 300) kW/m^2 . Bubbles diameter of (1.5 mm) was injected in the channel. The results showed heat transfer coefficients enhancement was mainly due to the secondary flow production. The rate of heat transfer was approximately 50 % higher than that for a single phase flow. **Tokuhiro, and Lykoudis, 1994**, investigated experimentally Nitrogen gas bubbles injection in mercury in a vertical enclosure. The vertical enclosure contained in one side a heated plate. The experiments were conducted using heat flux ranged $370 < q < 16000 W/mm^2$ and rate of bubble injection (0.9 to 9.2) cm^3/s . The results showed coefficient of heat transfer enhancement due to bubbles injection at low heat flux was more than that at higher heat fluxes. Also, heat transfer coefficient was approximately 2-3 times higher than that for a single phase flow, while at high heat fluxes, the influence of enhancement was not recognized. **Celata et al., 1999**, studied experimentally a turbulent upward mixed convection flow of water in a vertical pipe. Air injection was used to enhance heat transfer coefficient. Experiments had been carried out in a stainless steel tube with heat flux of (4.8 -178.5) kW/m^2 , Reynolds number (1160- 24000), liquid mass flow rate (80-850) Kg/h and gas mass flow rate (40-1800) g/h. Also, the flow pattern was illustrated by using plexiglas tube and prediction of the heat transfer coefficient by using correlation equations. The results showed that, gas phase caused secondary flow and disturbance in the velocity profile, therefore, turbulence increased locally by air bubbles effect which greatly enhanced the heat transfer coefficient. Also, results illustrated that the coefficient of heat transfer with injection of air bubbles was approximately 10 times higher than that for a single phase flow. **Wolters, 2003**, studied experimentally and numerically gas injection in mercury in vertical enclosure heated with constant heat flux in one side and cooled in other side. Thermocouples and double-conductivity probes were used to measure and calculate the local heat transfer and void fraction. The experiments were conducted using range of heat flux (370 to 16000) W/m^2 . The results showed a significant heat transfer enhancement was obtained during bubble injection utilization. For high heat fluxes the local Nusselt number was slightly decreased, probably because the effect of the stratified bulk fluid was decreased. The comparison between experimental and numerical results showed a reasonable agreement. **Kim, and Ghajar, 2006**, investigated experimentally the non-change phase of gas-liquid flow in horizontal pipes. Series of experiments had been carried out in order to clarify the flow pattern of heat transfer. The test section used in the experiments was made of stainless steel of (27.9 mm) inner diameter with ratio of length to diameter equals to (100). The experiments were conducted using range of heat flux (3000 to 10600) W/m^2 . The Reynolds numbers at (820-26000) for water and (560-48000) for air. The results cleared



that the rate of heat transfer increased with increasing Reynolds number. **Zimmerman et al., 2006**, investigated experimentally air bubble –water flows in a horizontal pipe. Superficial velocity (24.2-41.5) m/s for water and (0.02-0.09) m/s for air were utilized in the experiments. Speed video camera and conductive tomography technique were used to visualize flow patterns and measured film thickness. Infrared thermo-graphic method was used to measure temperature of the wall. The results showed that heat transfer coefficient at the bottom were higher than that at the top of the pipe. Also, local and average Nusselt number correlations were obtained. **Sakr et al., 2012**, studied numerically various turbulence models effect on turbulent bubbly flow through a vertical pipe and a pipe sudden expansion by using Eulerian's model. The momentum and continuity equations were used to describe the motion of flow. Different types of turbulence models: k- ϵ , extended k- ϵ and shear-stress transport k- ω turbulence models were implemented. Finite volume method was used to solve the equation of the system. Water was used as working fluid and air bubbles were used in this study. The water was used as a continuous phase while the air was represented as dispersed phase. The liquid Reynolds number of 78500 and bubble diameter of 2 mm were used in the experiments. It was concluded that, SST k- ω model plays an important role in comparison with other turbulence models. **Hameed, 2013**, investigated experimentally the effects of inclination angle of multiphase flow in pipe of square cross section. Inclination angles of 5°, 10°, and 15° were implemented. The following water and air superficial velocities of (1.1506 and 1.4815) m/s and (0.164 and 0.411) m/s were used in the experiments. The liquid Reynolds number was varied from (740 to 26000), and the gas Reynolds number was varied from (560 to 48000). Eight thermocouples type K distributed along the test section were used to measure the temperatures and to find local heat transfer coefficient. High speed camera was used to describe the flow regimes, along test section. The results showed that coefficient of heat transfer for multiphase flow increased with increasing flow rate of water, air, and inclination angle of test section. Correlation equations on average Nusselt number were obtained for three inclination angles of (5°, 10° and 15°). **Dizaji, and Jafarmadar, 2014**, investigated experimentally air injected flow into a liquid fluid of a horizontal double pipe heat exchanger to enhance heat transfer rate. Following conditions were based on, for cold water side of the heat exchangers: flow rate (0.083 kg/s), inlet temperature (25°C) and Reynolds number (4000), while for hot water side: inlet temperature (40°C), flow rate from (0.0831 to 0.2495) Kg/s, Reynolds number from (5000 to 16000) and air mass flow rate of (0.098×10^{-3}) Kg/s. The effects of air bubbles injected into the inner and outer tubes on heat exchanger were examined. The results showed that the presence of bubbles in outer tube of heat exchanger was more effective than that injected into the inner tube because of accumulation of air bubbles near the inner side of the outer tube. The maximum Nusselt number was about (6% - 35%) and effectiveness of heat exchanger was reached about (10%- 40%). **Hanafizadeh et al., 2014**, used two models, volume of fluid (VOF) and Eulerian for modeling air- water two- phase flow in up riser pipe for lift pump applications. CFD package was used to solve the conservation equations for two models. Different regimes through flowing gas-liquid flow in vertical pipes were observed: bubbly, slug, churn and annular. Conservation equations of mass and momentum were used in two directions (radial and axial). Effect of turbulence of the flow was computed by k- ϵ model. Test section was of (5cm) diameter and (1m) long. The results showed that for bubbly, slug and churn regimes were more appropriate for simulating by volume of fluid, while Eulerian's model was good for prediction of annular flow regime. **Sanati, 2015**, studied air bubble – water two phase flow in vertical pipe using k- ϵ model (mixture approach) and empirical correlations. The following conditions were used during the experimental work: superficial velocity (0.18 to 1.06) m/s and (0.03 to 3.1) m/s for water and air

respectively. The test section used in the experiments had different lengths (12.3 and 24) m under the same diameter. The two phase flow was governed by the Navier–Stokes equations, continuity equation and finite-volume method was used. Flow pattern and pressure distributions had been carried out in order to clarify the numerical results. It was concluded that the increasing in gas velocity was accompanied with increasing of void fraction which subsequently reduced total pressure loss in pipe but increased liquid velocity followed by reducing the void fraction and this led to increase of total pressure loss in pipe. Theoretical results showed agreement with the experimental results. **Rzehak, and Kriebitzsch, 2015**, investigated numerically turbulent bubbly flow through a vertical pipe. Both codes CFX and with OpenFOAM were used to simulate the results. Euler–Euler method was used in this model with turbulence model. Effect of bubbles on volume fraction of gas, velocity of liquid turbulent kinetic energy and turbulent viscosity were studied. It was concluded that, two codes peak value of gas volume fraction were predicted near the wall. Low value of profile for velocity was in the center and decreased to zero at the wall. Large value of turbulent kinetic energy was found by CFX code. Also, turbulent viscosity near the wall region had large value by CFX results. **Dabiri, and Tryggvason, 2015**, investigated numerically the effect of air bubbles on the turbulent upward flow between two parallel walls with a uniform heat flux. The following conditions were used during the experimental work: Reynolds number up to (5600) and bubble diameter (1.35mm). Series of experiments had been carried out in order to clarify the flow pattern on heat transfer coefficient and temperature distribution along vertical channel. The two-phase flow was governed by the Navier–Stokes equations, energy equation and finite-volume method was used for solution. They concluded that, an increase of (3%) in volume fraction of bubbles caused an increase of (60%) in Nusselt number.

The objective of the present work is to investigate numerically and experimentally the thermal effect of injecting air bubble in water flowing in vertical mounted pipe subjected to a uniform heat flux. Ranges of studied parameters are: water flow rate of (10, 14 and 18) lit/min, air flow rate of (1.5, 3, and 4) lit/min and heat fluxes (27264, 36316 and 45398) W/m². Numerical solution is carried out using a CFD code Fluent (Ansys15) and Gambit 2.2.30. Novelty of the this work is to measure the temperature of the liquid near the heated wall and the effect of air bubbles on Nusselt number in vertical circular pipe at constant heat flux numerically and experimentally.

2. EXPERIMENTAL WORKE

The experimental apparatus is shown photographically in **Fig.1** and diagrammatically in **Fig.2**. The test rig consists of the following items:

2.1 Test Section

The test section is a circular cross section channel manufactured from copper. The inside and outside diameters of the test section are (50mm) and (53mm) respectively. Test section length is (0.7m). Circular holes of (d=8 mm) are drilled in the surface of the cylinder. These holes are sealed by plugs of (d=8 mm) for penetration of thermocouple wires, pressure sensor and electric electrodes. The remained penetration areas are covered by silicon that withstands temperature up to 200°C. The outer tube surface was heated electrically using an electrical heater. The heater consists of two nickel-chrome wires of (1mm) in diameter, (3m) length. The wire is wrapped along its length around test section. The maximum power in each wire is (3000 W) ensuring total power of (6000 W). The bare wires of the heater are electrically insulated by Ceramic beads. The heater is supplied with AC-current from voltage regulator. The circuit is connected to digital voltage regulator to control the current according to the desired heat flux. Clamp meter is used to measure the current passing



through the heater. The heater is covered by a (2 in) layer of fiberglass that withstands temperature up to (700 - 850°C) to ensure a reliable insulation for the heater and to concentrate the generated heat in the water flowing inside test section. Aluminum plate covers the material. The temperature inside the test section is measured by thirty five thermocouples type K (chromium - aluminum) distributed within seven sections along the length of copper pipe. The thermocouples are installed in equal space (10 cm) apart at seven positions. Additional thermocouples are installed inside the tube to measure water temperature in the inlet and the outlet of the pipe as shown in **Fig. 3**. The end of thermocouple wires is connected with standard male plug in order to connect them with the digital thermometer. The system used to inject air bubbles in the test consists of (2 mm) diameter of capillary tube made of copper and compressor is used to provide the compressed air. The system is equipped with air flow meter and valve to control and measure the air bubbles generation rate.

2.2 Heat Exchanger (Double pipe helical coil)

Double pipe heat exchanger manufactured from copper is used in the present experiments. It consists of one pipe placed concentrically inside another pipe with larger diameter. The dimensions of the inner diameter and outer diameter are 1.6 cm and 2.3 cm respectively. The length of tube is 6m long. The purpose of the heat exchanger is to remove heat from outlet flow water of the test section and control water inlet temperature.

2.3 Pump

The water flowing in the circuit is divided between the test section and the bypass pipe. The purpose of the bypass pipe is to control water flow rate and pressure in the test section through a control valve. Another line is used in the circuit of heat exchanger to control the temperature of water enter test section.

2.4 Supply Liquid Water Tank

A water tank of (37 liter) with dimensions of (33x53x43) cm and (0.5 cm) plate thickness is placed at the same level of centrifugal pump and connected to the cold water inlet which is supplied from the water line in Laboratory.

2.5 Pipes and Valves

Polyvinyl chloride (PVC) pipe of (1/2 in) diameter is used to connect the parts of the system. The system consists of four valves.

3. MEASUREMENT AND CONTROL SYSTEMS

3.1 Electrical Power Measurement

- Voltage regulator (variance) is connected to the power supply for the purpose of adjusting the power input rate of the heater as required. A digital voltmeter is linked to the circuit in parallel with heater element to measure heater voltage.
- Hydrogen bubbles generation circuit consists of voltage regulator device (variance) and two multi-meter. Digital one is used to measure the current and the other is used to measure the output voltage from Variance.
- Digital watt meter is used to measure the heater power directly.
- Clamp multi-meter is used to measure the current passes through the heaters for cross checking.

3.2 Temperature Measurement

Digital thermometer type (12 channels temperature recorder with SD card data logger - model: BTM - 4208SD - Lutron Company - Taiwan) is used to measure the temperature.

4. HEAT TRANSFER CALCULATIONS

4.1 Heat Flux

The net heat flux is determined from recording the electrical power supplied to the heater and applying the following equation, **Salman, and Mohammed, 2007**:

$$P_o = I \cdot V_o \quad (1)$$

The heat transfer from the heated wall:

$$\Phi_{conv} = P_o - \Phi_{loss} \quad (2)$$

Where:

Φ_{loss} is the total conduction heat losses and radiation losses.

$$\Phi_{losses} = \Phi_{cond} + \Phi_{rad} \quad (3)$$

$\Phi_{radiation}$ is very small, so it can be neglected.

$$\Phi_{loss} = \frac{T_{wall} - T_{aluminum}}{\frac{\ln \frac{r_2}{r_1}}{2\pi\lambda_{pipe}L} + \frac{\ln \frac{r_3}{r_2}}{2\pi\lambda_{in.1}L} + \frac{\ln \frac{r_4}{r_3}}{2\pi\lambda_{in.2}L} + \frac{\ln \frac{r_5}{r_4}}{2\pi\lambda_{aluminum}L}} \quad (4)$$

The convection heat flux can be represented by:

$$q'' = \frac{\Phi_{conv}}{A_s} \quad (5)$$

Where: $A_s = \pi \times D_i \times L$

The bulk temperature profile along the length of tube can be represented by the following equation:

$$T_{b2}(x) = T_{b1} + \frac{q'' \cdot p \cdot x}{\dot{m} \cdot c_p} \quad (6)$$

The local heat transfer coefficient is expressed as:

$$h(x) = \frac{q''}{(T_{wall}(x) - T_{b2}(x))} \quad (7)$$

Average heat transfer coefficient

$$h = \frac{1}{x} \int_0^x h(x) dx \quad (8)$$

Local Nusselt number is calculated using following equation:

$$Nu(x) = \frac{h(x) D_i}{\lambda} \quad (9)$$

Average Nusselt number

$$Nu = \frac{1}{x} \int_0^x Nu(x) dx \quad (10)$$

The Reynolds number can be defined according to the particle diameter and the fluid velocity at the inlet as:

$$Re = \frac{\rho u D_i}{\mu} \quad (11)$$

4.2 Volume Fraction

Volume fraction in a gas-liquid flow may be defined as, **Kitagawa et al., 2008**:

$$\alpha = \frac{Q_{air}}{Q_{water} + Q_{air}} \quad (12)$$

4.3 Measurement of Air Bubble Diameter

The average initial bubbles size is elaborated by, **Azad, and Syeda, 2006**:

$$d_{airbubble} = d_c \left[1.88 \left(\frac{u_c}{\sqrt{g \cdot d_c}} \right)^{1/3} \right] \quad (13)$$

5. CFD SIMULATION

For multiphase, the Eulerian model approach was used to describe multiphase flow in three dimensions. Its approach treats the continuity, momentum, energy and equation of turbulence model for each phase, **Sakr et al., 2012**. The mathematical model was solved by using a CFD Code Fluent (Ansys15) and Gambit 2.2.30. The water was used as working fluid. Air bubbles injection was from two sides of pipe as shown in **Fig.4**.

Assumptions:

1. Steady and turbulent incompressible flow.
2. Three dimensional flows.
3. The properties of both gas and fluid were assumed to be constant.
4. Effect of surface tension were neglected.

With all the equations below for phase k (c: continuous and d: dispersed).

-The continuity equation (solved for each phase)

$$\frac{\partial}{\partial x_i} (\alpha \rho u_i)_k = 0.0 \quad (14)$$

The volume fractions were assumed to be equal to one.

$$\alpha_c + \alpha_d = 1.0 \quad (15)$$

- Momentum equation (solved for each phase)

$$\frac{\partial}{\partial x_i} (\alpha \rho u_i u_j)_k = -\alpha \frac{\partial P}{\partial x_i} \pm \alpha \rho g + \frac{\partial}{\partial x_j} \left[\alpha \mu \left(\frac{\partial u_i}{\partial x_j} + \frac{\partial u_j}{\partial x_i} - \frac{2}{3} \delta_{ij} \frac{\partial u_l}{\partial x_l} \right) \right]_k + \frac{\partial}{\partial x_j} (-\rho \dot{u}_i \dot{u}_j)_k \mp M_k \quad (16)$$

Where:

$$-\rho \dot{u}_i \dot{u}_j = \mu_t \left(\frac{\partial u_i}{\partial x_j} + \frac{\partial u_j}{\partial x_i} \right) - \frac{2}{3} \left(\rho k + \mu_t \frac{\partial u_k}{\partial x_k} \right) \delta_{ij} \quad (17)$$

Where:

$$\delta_{ij} = 1 \quad \text{if } i = j$$

$$\delta_{ij} = 0 \quad \text{if } i \neq j$$

The interface momentum transfer term M_k was given as follows, **Troshko, and Hassan, 2001, & Sakr et al., 2012**:

$$M_k = M_k^d + M_k^L + M_k^W + M_k^{td} \quad (18)$$

❖ The drag force was expressed as describes:

$$M_c^d = -M_d^d = \frac{3}{4} \frac{C_D}{d_b} \alpha_d \alpha_c |u_d - u_c| (u_d - u_c) \quad (19)$$

Where:

C_D = Drag coefficient depends on the particle Reynolds number as given below:

$$C_D = \begin{cases} \frac{24}{Re} (1 + 0.15 Re^{0.687}) & Re \leq 1000 \\ 0.44 & Re > 1000 \end{cases} \quad (20)$$



Relative Reynolds number was given by:

$$Re = \frac{\rho_c |u_d - u_c| d_b}{\mu_c} \quad (21)$$

❖ The lift force was expressed as:

$$M_c^L = -M_d^L = C_L \alpha_c \alpha_d \rho_c (u_d - u_c) \times (\nabla \times u_c) \quad (22)$$

Where:

C_L = Lift force coefficient

$C_L = 0.06$ (Turbulent bubbly flows in vertical pipes)

❖ Wall lubrication force was defined as:

$$M_c^W = -M_d^W = \frac{\alpha_c \alpha_d \rho_c |u_d - u_c|}{d_b} \max \left(0, C_{w1} + C_{w2} \frac{d}{y_w} \right) n_w \quad (23)$$

Where:

n_w = Outward vector normal to the wall.

y_w = Distance from the wall.

$C_{w1} = -0.01$

$C_{w2} = 0.05$

❖ The turbulent dispersion force was formulated as :

$$M_c^{td} = -M_d^{td} = -C_{td} \rho_c k_c \nabla \alpha_c \quad (24)$$

Where:

k_c = Turbulence kinetic energy of liquid per unit mass.

C_{td} = Coefficient of turbulent dispersion force ($C_{td} = 0.09$ to 0.1).

$\nabla \alpha_c$ = The gradient of dispersed volume fraction

- Energy equation (solved for each phase)

$$\frac{\partial}{\partial x_i} (\alpha \rho T u_i)_k = \alpha \left\{ \frac{\partial}{\partial x_i} \left[c_p \left(\frac{\mu}{\rho r} + \frac{\mu_t}{\sigma_t} \right) \frac{\partial T_i}{\partial x_j} \right] \right\}_k \quad (25)$$

-Turbulence modeling

The general transport equations for turbulence models adopted are given below, **Rzehak**, and **Kriebitzsch, 2015 & Dhotre, et al. 2007**:

-Turbulent kinetic energy

$$\frac{\partial}{\partial x_j} (\alpha \rho u_i K)_k = \frac{\partial}{\partial x_j} \left[\left(\mu + \frac{\mu_t}{\sigma_k} \right) \frac{\partial K}{\partial x_j} \right]_Z + \alpha (G_K - \rho \epsilon) + ST_K \quad (26)$$

-Turbulent dissipation rate

$$\frac{\partial}{\partial x_j} (\alpha \rho u \epsilon)_k = \frac{\partial}{\partial x_j} \left[\left(\mu + \frac{\mu_t}{\sigma_\epsilon} \right) \frac{\partial \epsilon}{\partial x_j} \right]_k + \alpha \left(\frac{c_{\epsilon 1} G_K \epsilon}{K} - \frac{c_{\epsilon 2} \epsilon^2 \rho}{K} \right) + ST_\epsilon \quad (27)$$

Where:

$$ST_K = C_{K3} C_f \rho_c \alpha_c \alpha_d K \quad (28)$$

$$ST_{\varepsilon} = C_{\varepsilon 3} C_f \rho_c \alpha_c \alpha_d \varepsilon \quad (29)$$

$$C_f = \frac{3}{4} \frac{C_D}{d_b} |u_d - u_c| \quad (30)$$

$$C_{K3} = 0.75$$

$$C_{\varepsilon 3} = 0.6$$

5.2 Mesh for Multiphase Flow

Three dimensional mesh generations as shown in **Figs.5** and **6**, was used for the air-water two-phase flow along a large vertical pipe. Air bubbles were used to inject in the water by small capillary tube with diameter (2mm) by two sides of the pipe. The mesh consisted of large vertical pipe and connected with another very small pipe mesh with dimension of (0.003 m) long and (0.002 m) in diameter for small capillary tube injected air bubbles. 347210 cells and 65220 nodes were used in the analysis.

6. RESULTS AND DISCUSSIONS

6.1 Results of the Two-Phase Flow (Numerical & experimental)

Fig.7 shows numerical results of temperature variation along the cylinder length and its radial distances at water flow rate (10 lit/min), heat flux (27264 W/m^2) and bubbles flow rates (1.5, 3 and 4 lit/min). The figures reveal that, water temperature increases along the length of cylinder with increasing distance from cylinder inlet and in the cylinder wall direction. The presence of air bubbles increases the velocity near the walls and reduces it in the center. The presence of bubbles increases the mixing (cold water and warm water) and thus reduces the temperature differences between the wall and the bulk water. Experimental results illustrated in **Fig.8** shows the difference with numerical results due to the influence of losses through experimental test and accuracy of measuring device.

Fig.9 shows numerical and experimental results of bulk temperature variation with dimensionless length of cylinder at different water flow rates (10, 14 and 18) lit/min, heat fluxes (27264 and 36316 W/m^2) and bubbles flow rates (0, 1.5, 3 and 4) lit/min. It is obvious from the figure that at constant heat flux, the bulk temperature is inversely proportional to water flow rate as this temperature decreases by increasing Reynolds number. Also, the observed cases show that, mixing increases by bubbles increases the bulk temperature. The behavior of experimental results of bulk temperature is similar to those related to numerical results but with increased values. Similar trends were shown for heat flux 36316 W/m^2 .

Fig.10 shows the results of wall temperature variation with dimensionless length of cylinder with different values of water flow rates (10, 14 and 18) lit/min, heat fluxes (27264 and 36316 W/m^2) and bubbles flow rates (0, 1.5, 3 and 4) lit/min. It illustrates that the wall temperature in the case of injection air bubbles is much lower than that in the case of without bubbles because bubbles increase mixing between hot and cold streams. From numerical results, at heat flux (27264 W/m^2), maximum reduction of wall temperature was 29% at water flow rates (10) lit/min and bubbles flow rate (4 lit/min), while maximum reduction 20% for the same conditions was found in experimental test.

Fig.11 shows the results of local Nusselt number variation with length of cylinder for different values of water flow rates, heat fluxes and bubbles flow rates. The results show that bubbles injection causes secondary flow and disturbance in the velocity profile which increases turbulence locally by air bubbles effect and enhance the local Nusselt number. For the same heat flux the local Nusselt number value increases as the rate of bubbles injection increases. From numerical results, it



was noticed that, at heat flux (27264 W/m^2) local Nusselt number increased 31% when bubbles flow rate (4 lit/min), while it increased 17% at minimum value of bubbles flow rate (1.5 lit/min) for the same value of water flow rates (10) lit/min. Level of increased local Nusselt number from experimental results is more than numerical results.

Fig.12 shows the results of average Nu variation versus Re at different values of heat fluxes and air bubbles flow rates. The effect of secondary flow by bubbles injection is significant at lower heat fluxes and lower flow rates. As seen from this figures, the secondary flow by air bubbles injection causes increase in average Nusselt number as Reynolds number decreases. Also the average Nu number increases as bubbles flow rates increases. The enhancement related to the average Nusselt number is shown in **Table 1**.

The variation of ratio of average Nu_o/Nu with Re number at heat flux 27264 W/m^2 is shown in **Fig.13a**. The ratio decreases with Re number increase, because bubble motion moves away from the wall. It illustrates that an increase in air bubbles injection rate causes an increase in the average Nu_o/Nu ratio. Also, the results show a similar trend obtained for $q''=36316 \text{ W/m}^2$ and $q''=45398 \text{ W/m}^2$, however, the ratio of average Nu_o/Nu decreases as heat flux increases.

Comparison of present work was made for two phase flow with the work of **Celata et al., 1999**, which was considered to be the best one to compare as shown in **Fig.14** and a good agreement was observed.

6.2 Correlations of Average Nusselt Number

The correlation of average Nusselt number (Nu) with (Ra/Re) that covers the experimental results:

$$Nu = c(Ra/Re)^n \quad (31)$$

Where c and n are empirical constants. Each of these constant is presented in **Table 2** for range of: (Re = 5269 to 10528 and Gr= 1.42×10^8 to 2.39×10^{10})

7. CONCLUSIOS

1. The difference between experimental and numerical results was due to the influence of losses through experimental test and accuracy of measuring devices.
2. The enhancement of average Nusselt number ratio with effect of air bubbles to that without bubbles increased from (1.02 to 1.32).
3. Air bubbles injection causes an increase in average Nusselt number with increases in Reynolds number.
4. The high rate of bubbles injection had more effect on heat transfer enhancement.
5. A reduction in wall temperature along test section by injection bubbles increases with increasing the rate of bubble injection.
6. New correlation equations of Nusselt number were obtained from experimental results
7. Reasonable agreement was obtained between measured temperature and theoretical temperature predictions by CFD code.

8. REFERENCES

- Azad, M. A. K., and Syeda, S, R., 2006, *A Numerical Model for Bubble Size Distribution in Turbulent Gas- Liquid Dispersion*, Journal of Chemical Engineering, IEB. Vol.24, No.1, PP.25-34.



- Celata, G. P., Chiaradia, A., Cumo, M., and DAnnibale, F. , 1999, *Heat Transfer Enhancement by Air Injection in Upward Heated Mixed-Convection Flow of Water*, Journal of Multiphase Flow, Vol.25, PP.1033-1052.
- Dizaji, H.S., and Jafarmadar, S., 2014, *Heat Transfer Enhancement Due to Air Bubble Injection into a Horizontal Double Pipe Heat Exchanger* , International Journal of Automotive Engineering ,Vol. 4, No. 4,PP.902-910.
- Dabiri , S., and Tryggvason, G., 2015, *Heat Transfer in Turbulent Bubbly Flow in Vertical Channels*, Journal of Chemical Engineering Science, Vol. 122,No. 27, PP. 101- 113 .
- Dhotre, M.T, Smith,B.L., and Niceno.,B.,2007,*CFD Simulation of Bubbly Flows: Random Dispersion Model*,Journal of Chemical Engineering Science Vol.62, PP.7140-7150.
- Hanafizadeh, P., Moezzi, M., and Saidi, M. H., 2014,*Simulation of Gas-Liquid Two Phase Flow in Upriser Pipe of Gas-Lift Systems*, Energy Equipment and Systems, Vol 2,PP. 25-41 .
- Hameed ,R. H., 2013, *Experimental Investigation of Heat Transfer to Air–Water Flow in Downward Inclined Square Pipe*,Thi-Qar University, Journal for Engineering Sciences, Vol. 4, No. 1,PP. 1-15.
- Kim, J. Y., and Ghajar , A. J., 2006, *A General Heat Transfer Correlation for Non-Boiling Gas–Liquid Flow with Different Flow Patterns in Horizontal Pipes*, International Journal of Multiphase Flow,Vol. 32,PP. 447–465.
- Kitagawa , A., Kosuge , K., Uchida, K., and Hagiwara,Y.,2008,*Heat Transfer Enhancement for Laminar Natural Convection Along a Vertical Plate Due to Sub-Millimeter-Bubble Injection*, Journal of Experiments in Fluids, Vol. 45, PP. 473–484.
- Kenning ,D. B. R. and Kao, Y. S., 1972,*Convection Heat Transfer to Water Containing Bubbles Enhancement Not Dependent on Thermocapillarity*, International Journal of Heat and Mass Transfer, Vol.15, pp.1709-1717.
- Rzehak,R., and Kriebitzsch. S., 2015, *Multiphase CFD-Simulation of Bubbly Pipe Flow: A Code Comparison*,International Journal of Multiphase Flow,Vol.68 , PP.135-152.
- Sakr, I.M., El-Askary, W.A., Balabel, A. and Ibrahim, K., 2012, *Computations of Upward Water/Air Fluid Flow in Vertical Pipes*, CFD Letters, Vol. 4, No.4, PP. 193-213.
- Sanati, A., 2015,*Numerical Simulation of Air–Water Two–Phase Flow in Vertical Pipe Using K-E Model*, International Journal of Engineering& Technology, Vol.4 ,No.1,PP. 61-70.



- Salman, Y. K., and Mohammed, H.A., 2007, *Free Convective Heat Transfer with Different Sections Lengths Placed at the Exit of a Vertical Circular Tube Subjected to a Constant Heat Flux*, Journal of Al-Khwarizmi Engineering, Vol.3, No.3, pp. 31-52.
- Tokuhiko, A.T., Lykoudis, P.S., 1994, *Natural Convection Heat Transfer From a Vertical Plate-I. Enhancement with Gas Injection*, International Journal of Heat Mass Transfer, Vol.37, No.6, PP.997–1003.
- Troshko, A. A., and Hassan, Y. A., 2001. *Two Equations Turbulence Model of Turbulent Bubbly Flow*, International Journal of Multiphase Flow, Vol. 27, PP.1965-2000.
- Wolters, J., 2003, *Benchmark Activity on Natural Convection Heat Transfer Enhancement in Mercury with Gas Injection*, ZAT-Report No. 379, PP. 1-54.
- Zimmerman, R., Gurevich, M., Mosyak, A., Rozenblit, R., and Hetsroni, G., 2006, *Heat Transfer to Air–Water Annular Flow in a Horizontal Pipe*, International Journal of Multiphase Flow, Vol. 32, PP. 1-19.

9. NOMENCLATURE

Symbols

A = area of cross section, m^2

A_s = surface area, m^2

$C_\mu, C_{\epsilon 1}, C_{\epsilon 2}$ = constants in turbulence model, dimensionless

C_D = drag coefficient, dimensionless

C_L = lift force coefficient, dimensionless

C_{td} = turbulent dispersion force constant, dimensionless

C_{w1}, C_{w2} = constants in wall lubrication force, dimensionless

D_i = tube inner diameter, m

D_o = tube outer diameter, m

$d_{airbubble}$ = diameter of capillary tube of air bubble, m

d_c = diameter of capillary tube, m

g = gravitational acceleration, N/m^2

K = turbulent kinetic energy, dimensionless

k = number of phases, dimensionless

L = length of pipe, m

M_k = interface momentum transfer, N

M_k^d = drag force, N

M_k^L = lift force, N

M_k^W = turbulent dispersion force, N

n_w = outward unit vector is perpendicular to the wall, dimensionless

P = pressure, Pa

P_o = electrical power, W

Nu = average Nusselt number, dimensionless



N_{ux} = local Nusselt number, dimensionless
 T_{in} = inlet temperature, °C
 T_{wall} = wall temperature, °C
 $T_{aluminum}$ = aluminum temperature, °C
 T_{b1} = bulk temperature at inlet, °C
 T_{b2} = bulk temperature at outlet, °C
 T_{bulk} = bulk temperature, °C
 u_c = air velocity through the capillary tube, m/s
 R, X, θ = cylindrical coordinates
 V_o = voltage, Volt

Greek Symbols

α = volume fraction, dimensionless
 ε = dissipation rate of turbulent kinetic energy, dimensionless
 λ = thermal conductivity, (W/m.°C)
 ϕ_{conv} = convection of heat transfer, W
 ϕ_{loss} = loss of heat transfer, W
 ϕ_{cond} = conduction heat transfer, W

Table 1. Value of enhancement average Nueeslt number.

q'' W/m ²	Re	Numerical results			Experimental results		
		Q_{air} (lit/min)			Q_{air} (lit/min)		
		1.5	3	4	1.5	3	4
27264	5269	12%	25.2%	33.4%	11.1%	19%	26%
	7377	11%	23.6%	31%	10.4%	18%	24.2%
	10528	9%	21.2%	30%	10%	17%	23.5%
36316	5269	8.3%	17%	28%	11.2%	18.4%	25.5%
	7377	7.1%	16.3%	26.2%	10.2%	15.3%	24%
	10528	6.4%	14.7%	24.3%	7.6%	13.45	23%
45398	5269	6.7%	15%	26.4%	9%	16.5%	24.4%
	7377	5.4%	13%	23.4%	8.3%	14.3%	22.2%
	10528	4.6%	11%	22.1%	7.3%	12.3%	20.7%

Table 2. Correlations of the average Nusselt number as a function of Ra/Re.

q'' (W/m ²)	Q_{air} (lit/min)	Correlation equation
27264	0.0	$Nu=3.366 (Ra/Re)^{-0.35}$
	1.5	$Nu=4.020 (Ra/Re)^{-0.45}$
	3	$Nu=3.404(Ra/Re)^{-0.33}$
	4	$Nu=6.177 (Ra/Re)^{-0.70}$
36318	0.0	$Nu=5.761 (Ra/Re)^{-0.67}$
	1.5	$Nu=3.872 (Ra/Re)^{-0.41}$
	3	$Nu=3.711(Ra/Re)^{-0.38}$
	4	$Nu=4.229 (Ra/Re)^{-0.45}$
45398	0.0	$Nu=5.68 (Ra/Re)^{-0.57}$
	1.5	$Nu=4.553 (Ra/Re)^{-0.45}$
	3	$Nu=5.277(Ra/Re)^{-0.52}$
	4	$Nu=6.394 (Ra/Re)^{-0.62}$



Figure 1. Photograph of experimental apparatus.

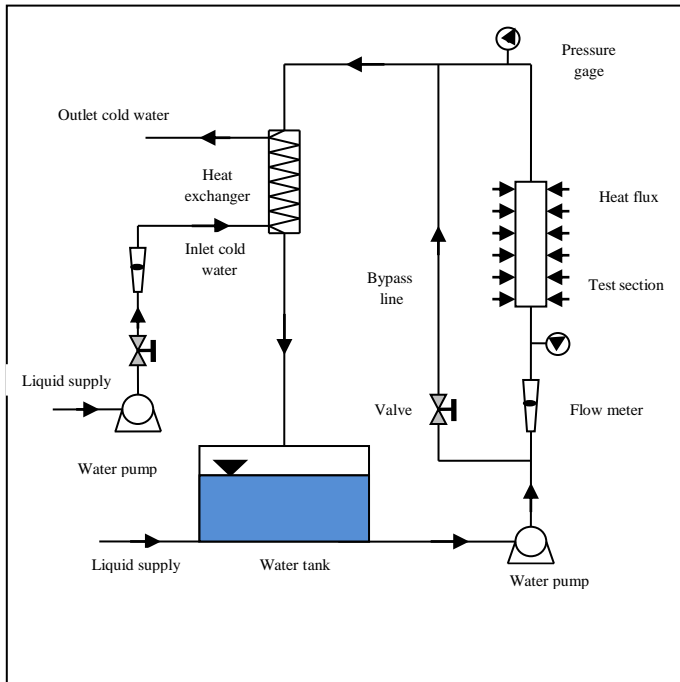


Figure 2. Schematic diagram of the experimental apparatus.

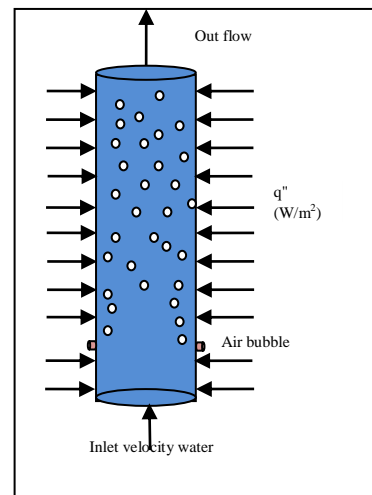


Figure 3. Test section layout with air bubbles injection.

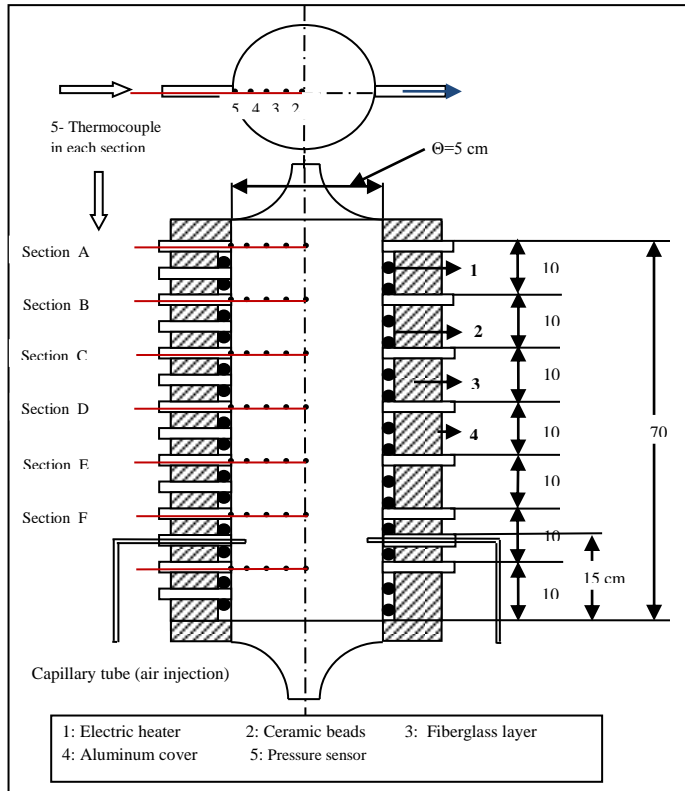


Figure 4. Geometry of pipe in three Dimensions with air bubbles injection

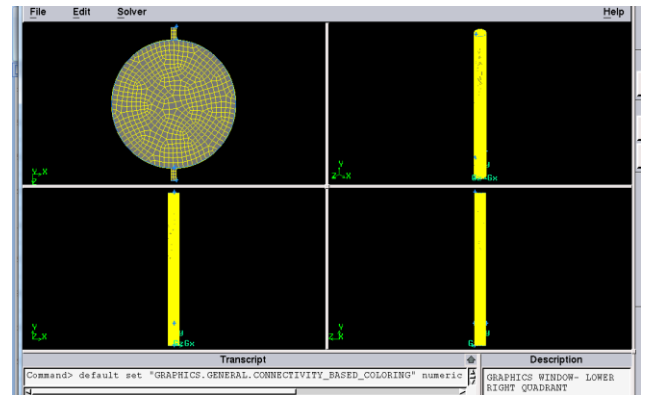


Figure 5. Mesh for multiphase turbulent flow in pipe.

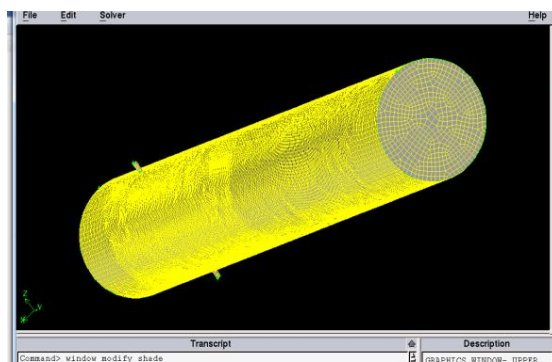
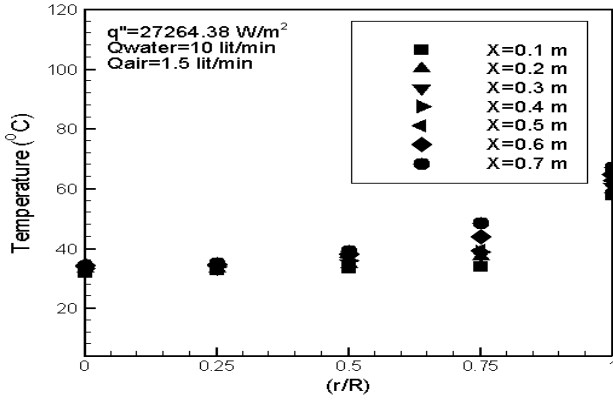
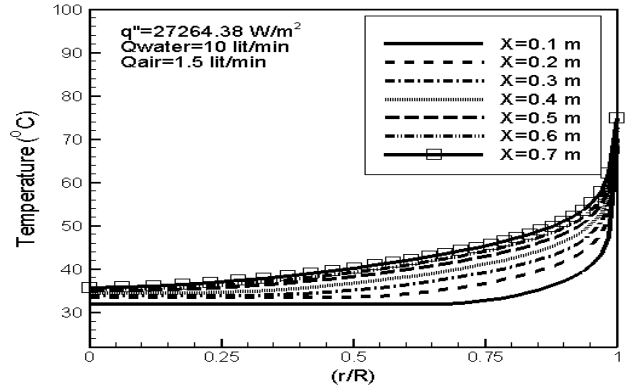


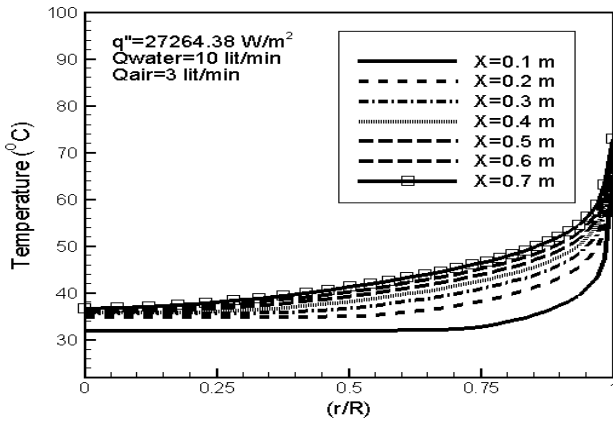
Figure 6.Continued.



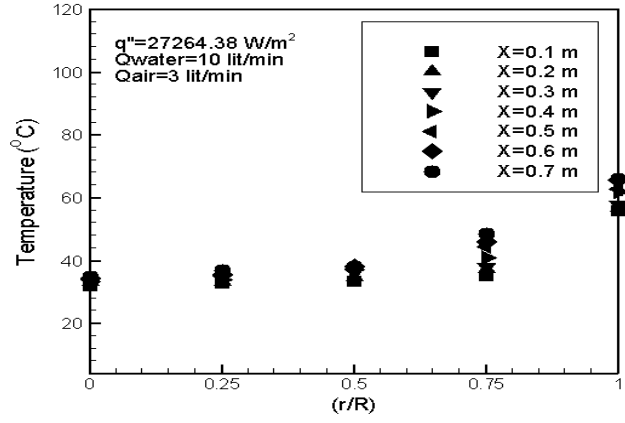
(a) $q'' = 27264 \text{ W/m}^2$



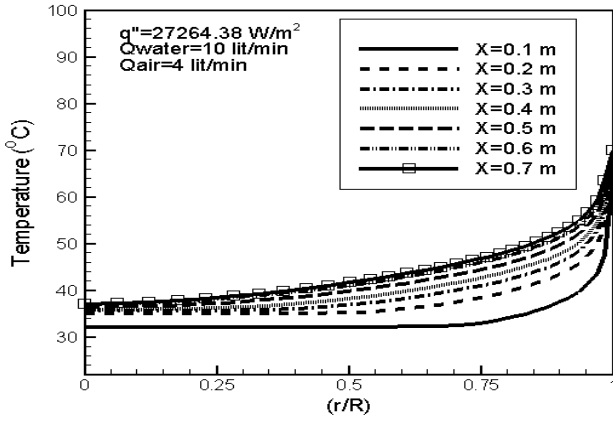
(a) $q'' = 27264 \text{ W/m}^2$



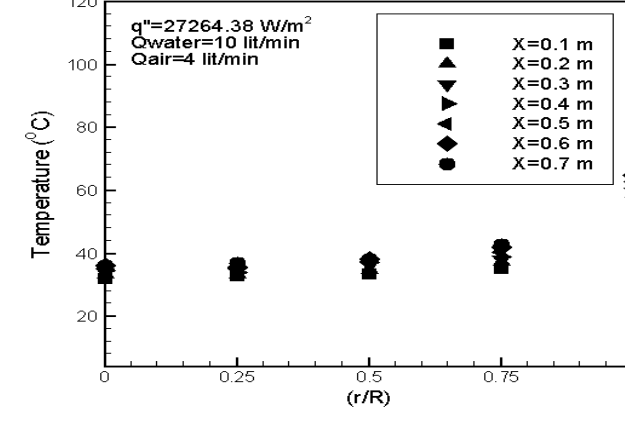
(b) $q'' = 27264 \text{ W/m}^2$



(b) $q'' = 27264 \text{ W/m}^2$



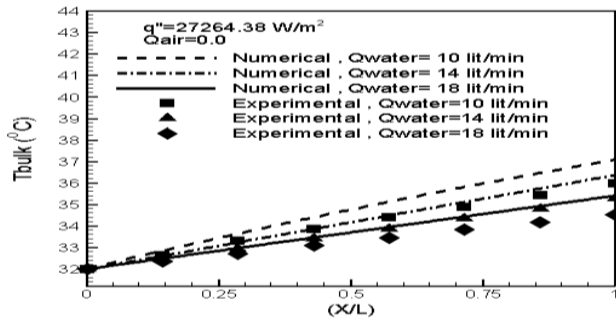
(c) $q'' = 27164 \text{ W/m}^2$



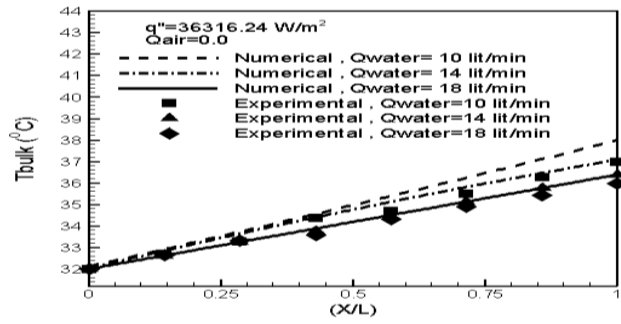
(c) $q'' = 27264 \text{ W/m}^2$

Figure 7. Numerical results of temperature variation with cylinder radial distance for different flow rates and rate of heat fluxes at $q''=27264 \text{ W/m}^2$

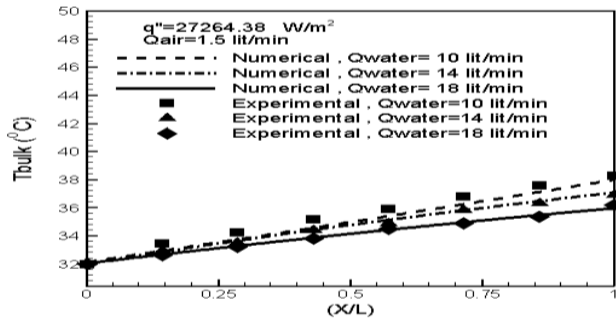
Figure 8. Experimental results of temperature variation with cylinder radial distance for different flow rates and rate of heat fluxes at $q''=27264 \text{ W/m}^2$.



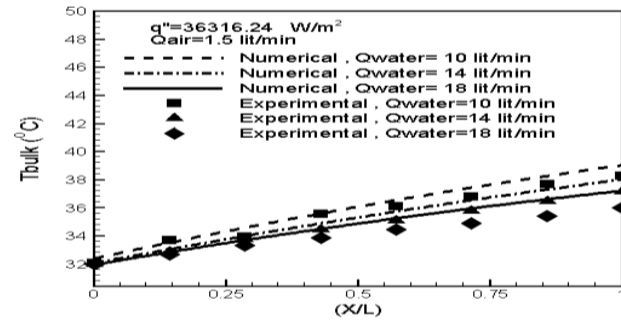
(a) $q'' = 27264 \text{ W/m}^2$



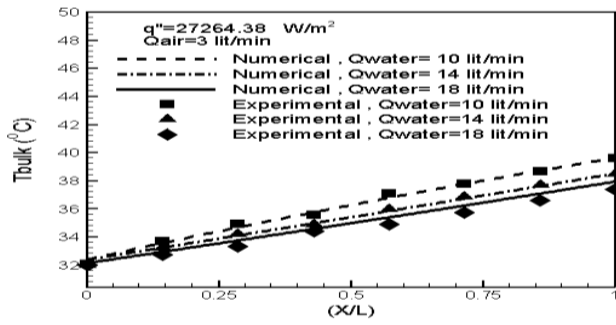
(a) $q'' = 36316 \text{ W/m}^2$



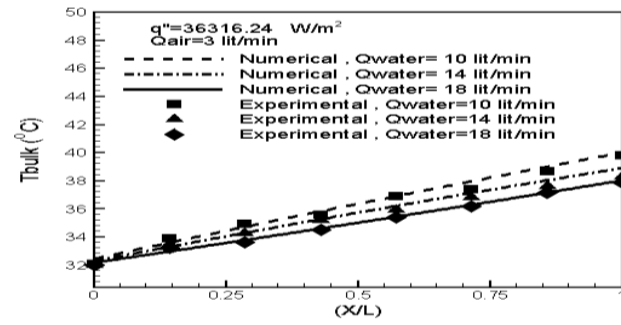
(b) $q'' = 27264 \text{ W/m}^2$



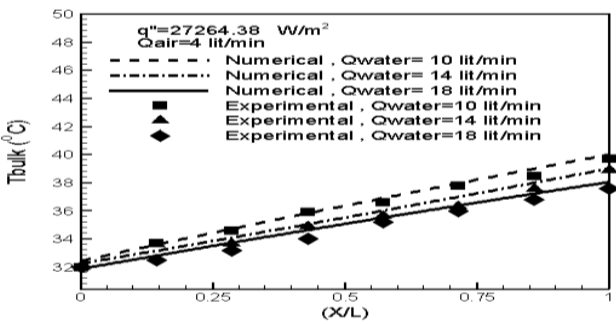
(b) $q'' = 36316 \text{ W/m}^2$



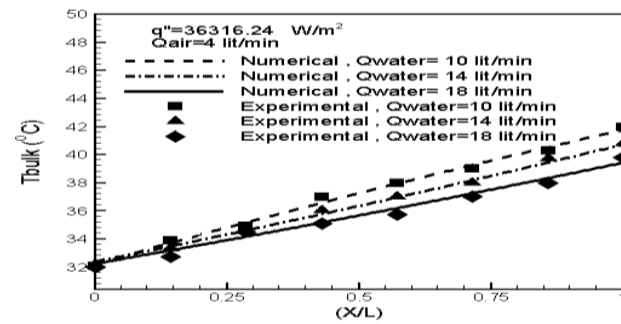
(c) $q'' = 27264 \text{ W/m}^2$



(c) $q'' = 36316 \text{ W/m}^2$

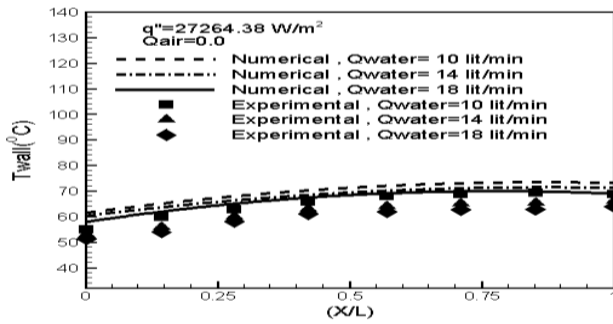


(d) $q'' = 27264 \text{ W/m}^2$

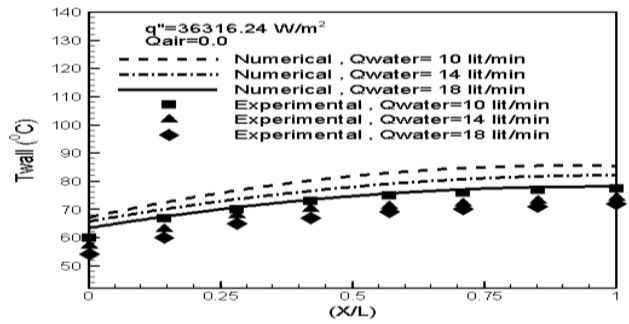


(d) $q'' = 36316 \text{ W/m}^2$

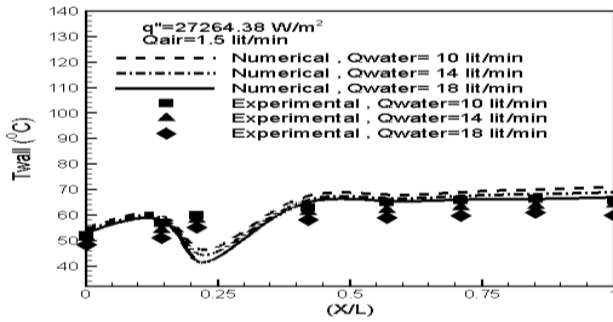
Figure 9. Comparison of numerical and experimental results of bulk temperature variation with length of cylinder for different values of heat fluxes.



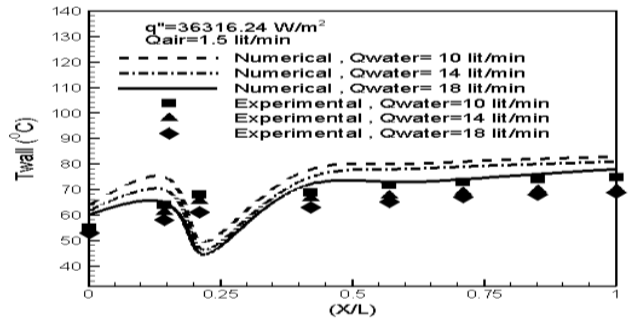
(a) $q'' = 27264 \text{ W/m}^2$



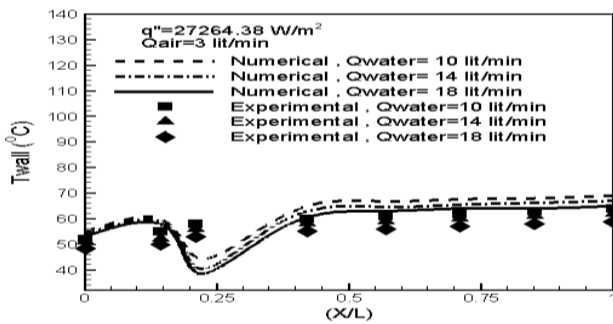
(a) $q'' = 36316 \text{ W/m}^2$



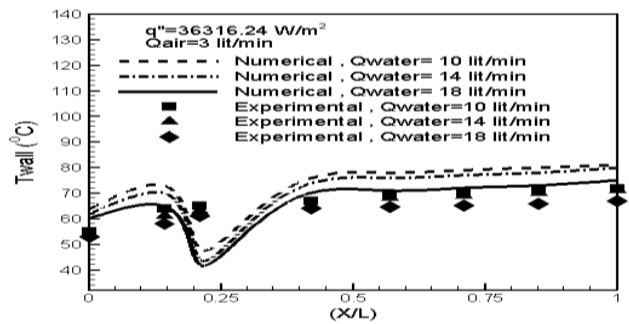
(b) $q'' = 27264 \text{ W/m}^2$



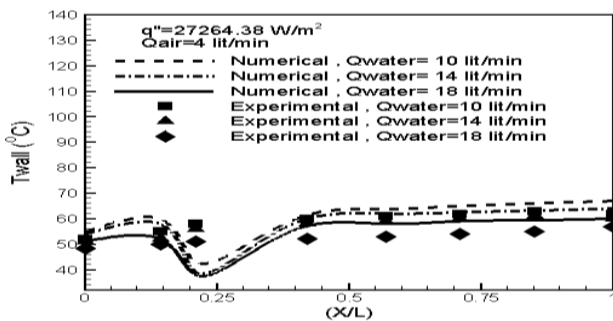
(b) $q'' = 36316 \text{ W/m}^2$



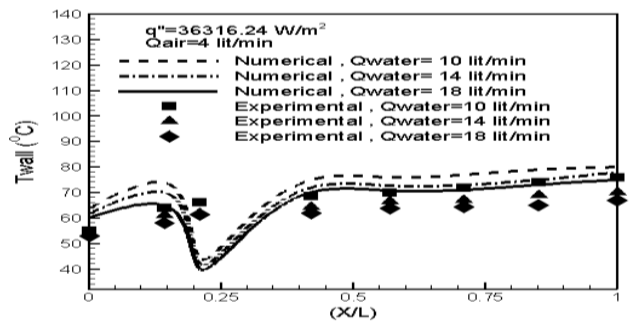
(c) $q'' = 27264 \text{ W/m}^2$



(c) $q'' = 36316 \text{ W/m}^2$

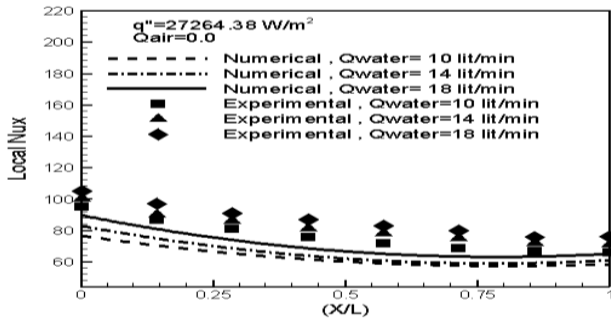


(d) $q'' = 27264 \text{ W/m}^2$

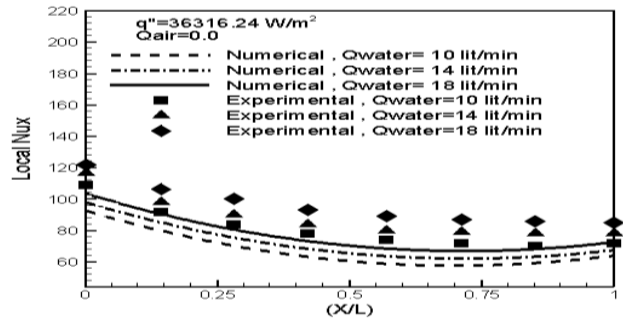


(d) $q'' = 36316 \text{ W/m}^2$

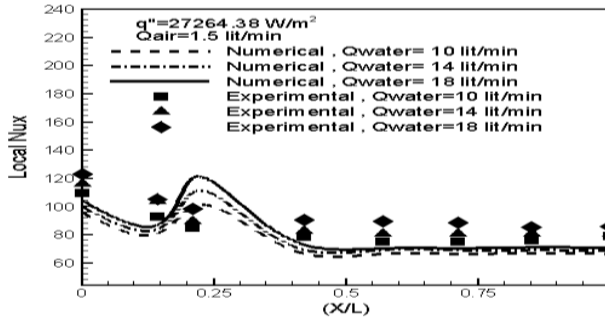
Figure 10. Comparison of numerical and experimental results of wall temperature variation with length of cylinder for different values of heat fluxes.



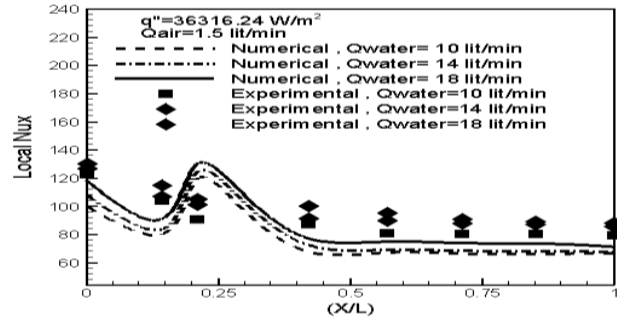
(a) $q'' = 27264 \text{ W/m}^2$



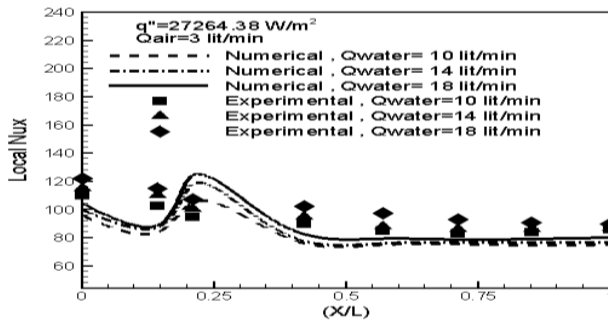
(a) $q'' = 36316 \text{ W/m}^2$



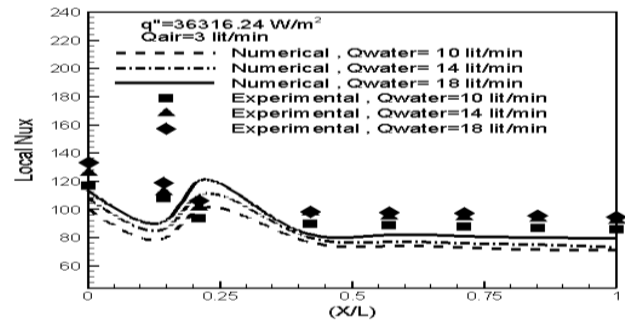
(b) $q'' = 27264 \text{ W/m}^2$



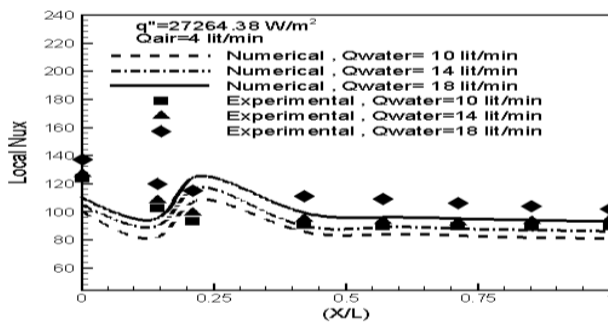
(b) $q'' = 36316 \text{ W/m}^2$



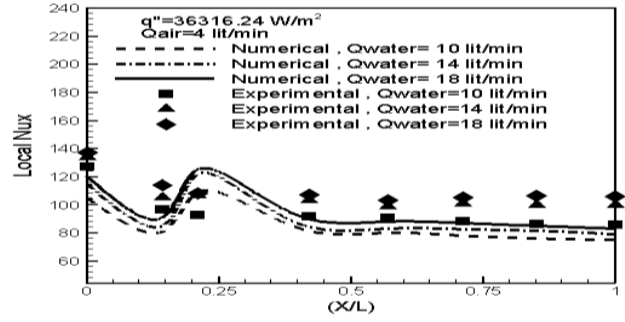
(c) $q'' = 27264 \text{ W/m}^2$



(c) $q'' = 36316 \text{ W/m}^2$

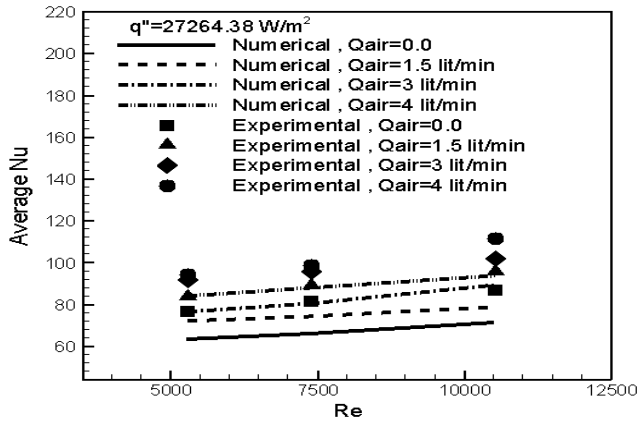


(d) $q'' = 27264 \text{ W/m}^2$

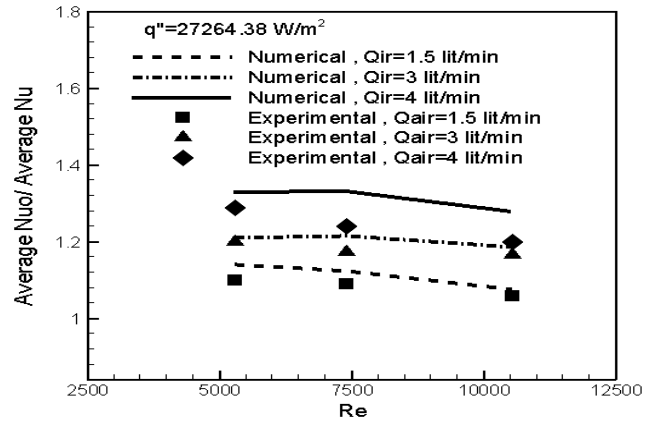


(d) $q'' = 36316 \text{ W/m}^2$

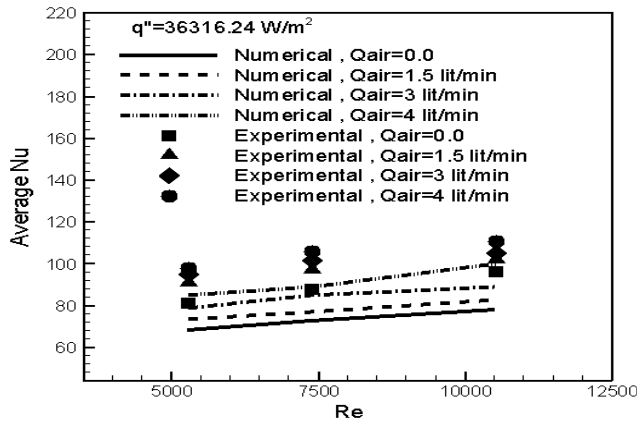
Figure 11. Comparison of numerical and experimental results of local Nusselt number variation with length of cylinder for different values of heat fluxes.



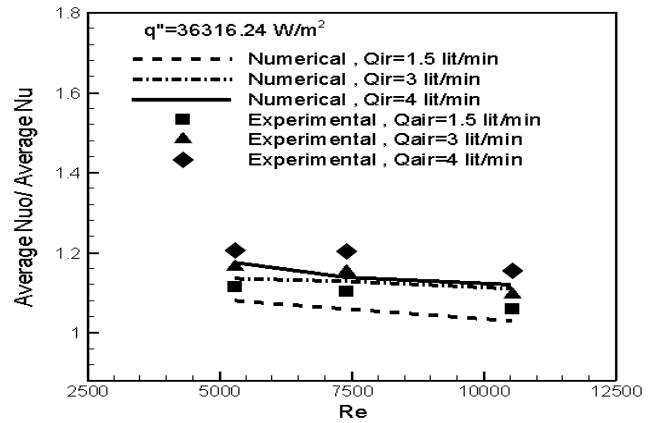
(a) $q'' = 27264 \text{ W/m}^2$



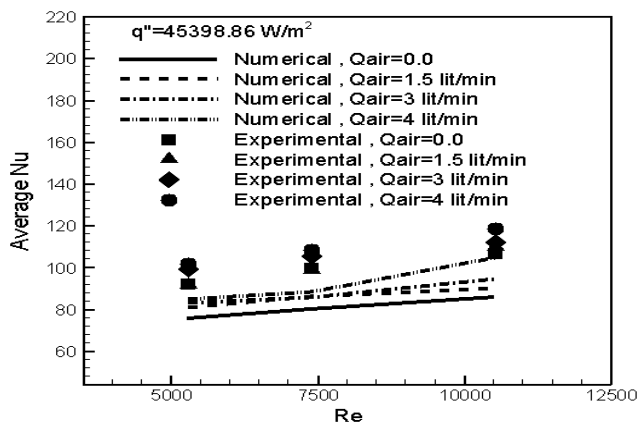
(a) $q'' = 27264 \text{ W/m}^2$



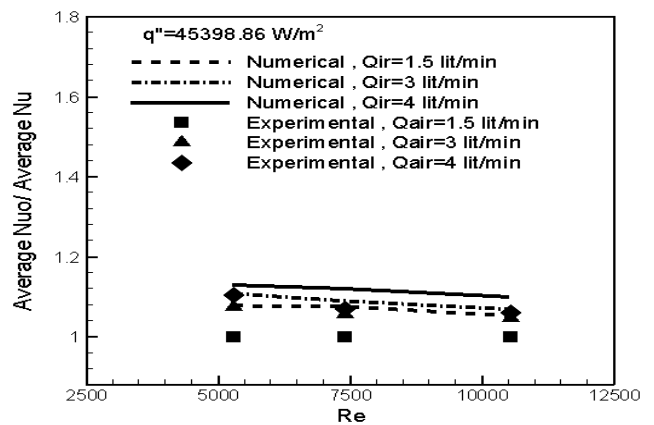
(b) $q'' = 36316 \text{ W/m}^2$



(b) $q'' = 36316 \text{ W/m}^2$



(c) $q'' = 45398 \text{ W/m}^2$



(c) $q'' = 45398 \text{ W/m}^2$

Figure12.Experimental results of average Nu number variation with Re number at different values of heat flux and Q_{air} .

Figure13.Experimental results of ratio of average Nu_0/Nu variation with Re number at different values of heat flux and Q_{air} .

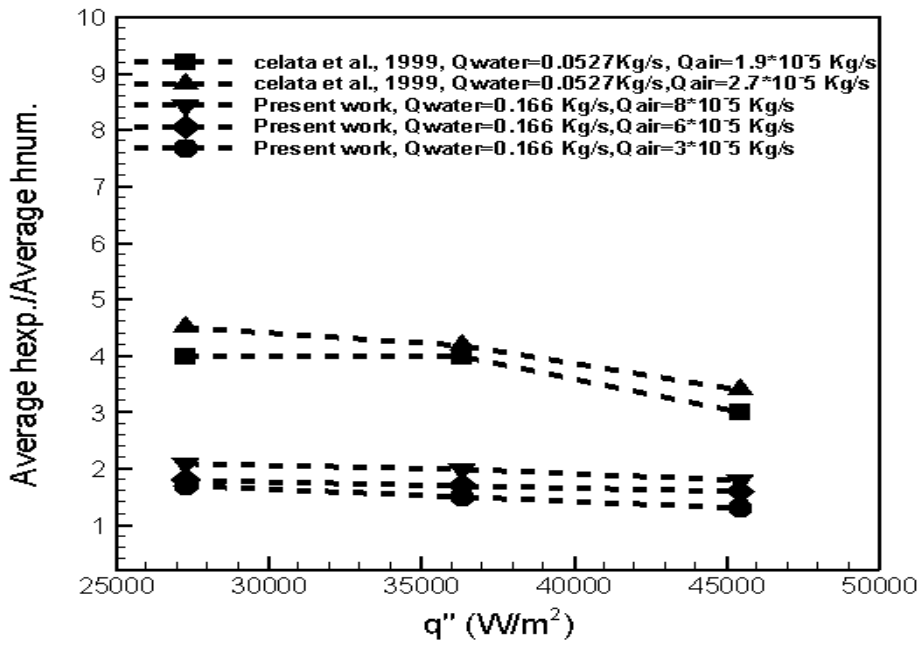


Figure 14. Comparison of the experimental and numerical results of ratio average h experimental / average h numerical for two phase flow with, **Celata et al., 1999**.